JACC Vol. 28, No. 5
November 1, 1996:1292–300

Hemodynamic Characteristics, Myocardial Kinetics and Microvascular Rheology of FS-069, a Second-Generation Echocardiographic Contrast Agent Capable of Producing Myocardial Opacification From a Venous Injection

DANNY M. SKYBA, PhD, GUSTAVO CAMARANO, MD, NORMAN C. GOODMAN, BS, RICHARD J. PRICE, PhD, THOMAS C. SKALAK, PhD, SANJIV KAUL, MD, FACC

Charlottesville, Virginia

Objectives. **We sought to 1) study the effects of FS-069 on cardiac and systemic hemodynamic function, myocardial blood flow, left ventricular wall thickening and pulmonary gas exchange when injected intravenously; and 2) compare the myocardial kinetics and microvascular rheology of FS-069 and Albunex when injected directly into a coronary artery.**

Background. **FS-069 is a second-generation echocardiographic contrast agent composed of perfluoropropane-filled albumin microspheres; it is capable of consistent and reproducible myocardial opacification from a venous injection.**

Methods. **Nine dogs were used to study the effects of FS-069 on hemodynamic function, pulmonary gas exchange, left ventricular wall thickening and myocardial blood flow and to characterize its myocardial kinetics when injected intravenously. These dogs were also used to compare the myocardial kinetics of FS-069 with those of Albunex during intracoronary injections. Nine Sprague-Dawley rats were used to compare the microvascular rheology of these two contrast agents, and in vitro modeling was performed to assess whether the microvascular findings of FS-069 can explain its echocardiographic behavior during direct coronary injections.**

Results. **There were no effects of 30 rapid venous injections of FS-069 (every 20 s) on cardiac output; mean aortic, pulmonary or left atrial pressures; and peak positive and negative first derivative of left ventricular pressure (dP/dt). Similarly, there were no effects of this agent on radiolabeled microsphere–measured regional myocardial blood flow, left ventricular wall thickening or pulmonary gas exchange. When injected intravenously, the myocardial transit of this agent resembled a gamma-variate form. When diluted FS-069 was injected directly into the coronary artery; however, its transit resembled the integral of gamma-variate function, with persistent myocardial opacification lasting several minutes, which was different from that of Albunex. Intravital microscopy revealed that, unlike Albunex, when no bubbles are entrapped within the microcirculation after an arterial injection, a very small fraction of the diluted, larger FS-069 microbubbles are entrapped. In vitro modeling confirmed that this small fraction of microbubbles can result in persistent myocardial opacification.**

Conclusions. **FS-069 produces no changes in hemodynamic function, myocardial blood flow, left ventricular wall thickening or pulmonary gas exchange when injected intravenously in large amounts. When diluted FS-069 is injected into the coronary artery, a very small fraction of the larger bubbles are entrapped within the microcirculation, resulting in a persistent contrast effect. Thus, although FS-069 is a safe intravenous echocardiographic contrast agent, it cannot provide information on myocardial blood flow when injected directly into a coronary artery.**

(J Am Coll Cardiol 1996;28:1292–300)

Although several clinical applications have been described for myocardial contrast echocardiography, they have been limited to the cardiac catheterization laboratory (1–9) and the operating room (8,9) because of the unavailability of echocardiographic contrast agents capable of consistently producing myocardial opacification from a venous injection. A major limitation of the first-generation echocardiographic contrast agents, such as Albunex, is that they contain air, which is highly diffusible and rapidly escapes from the bubbles when mixed with blood (10). Because the backscatter of a bubble is related exponentially to its radius (11), loss of air with a consequent decrease in bubble size results in a decrease in its backscattering properties. This limitation has been overcome in the

From the Cardiovascular Division and the Department of Biomedical Engineering, University of Virginia, Charlottesville, Virginia. This study was supported in part by Grants R01-HL48890, R01-HL-39680 and R01-HL-49146 from the National Heart, Lung, and Blood Institute, National Institutes of Health, Bethesda, Maryland; a grant from Molecular Biosystems, Inc., San Diego, California; and an equipment grant from General Electric Medical Systems, Milwaukee, Wisconsin. Dr. Camarano was the recipient of a Fellowship Training Grant from Mallinckrodt Medical, Inc., Saint Louis, Missouri. Dr. Price is the recipient of a Postdoctoral Training Grant from the Virginia Affiliate of the American Heart Association, Glen Allen, Virginia. Dr. Kaul is an Established Investigator of the National Center of the American Heart Association, Dallas, Texas. This study was presented in part at the 5th and 7th Annual Scientific Sessions of the American Society of Echocardiography, San Francisco, California, June 1994 and Chicago, Illinois, June 1996, respectively.

Manuscript received April 15, 1996; revised manuscript received June 20, 1996, accepted July 1, 1996.

Address for correspondence: Dr. Sanjiv Kaul, Cardiovascular Division, Box 158, Medical Center, University of Virginia, Charlottesville, Virginia 22908.

Published by Elsevier Science Inc.

0735-1097/96/$15.00
PII S0735-1097(96)00328-2

Abbreviations and Acronyms

dP/dt = first derivative of left ventricular pressure
DTAF = 5-[(4,6-dichlorotriazin-2-YL)amino]-fluorescein
ECG = electrocardiogram, electrocardiographic

second-generation contrast agents by use of high molecular weight gases such as perfluorocarbons (10). These gases do not diffuse out of the microbubbles as readily, resulting in maintenance of their original size and backscattering properties.

FS-069 is one of the new second-generation contrast agents consisting of sonicated albumin microspheres filled with perfluoropropane, which is capable of consistent myocardial opacification from a venous injection (12,13). The main aim of this study was to determine the effect of this new agent on hemodynamic function, myocardial blood flow, left ventricular wall thickening and pulmonary gas exchange when injected intravenously. A second aim of this study was to compare the myocardial kinetics and microvascular rheology of FS-069 with those of Albunex when injected directly into a coronary artery.

Methods

The experiments were approved by the Animal Research Committee at the University of Virginia and conformed to the "Position of the American Heart Association on Research Animal Use" adopted by the Association in November 1984. Nine adult mongrel dogs and nine Sprague-Dawley rats were used for the experiments. The dogs were used to assess the effect of FS-069 on hemodynamic function, pulmonary gas exchange, left ventricular wall thickening and myocardial blood flow, as well as to characterize its myocardial kinetics when injected intravenously. The animals were also used to compare the myocardial kinetics of diluted FS-069 to those of Albunex after a bolus injection directly into a coronary artery. Intravital microscopy was performed in nine Sprague-Dawley rats to compare the microvascular rheology of these two contrast agents, and in vitro modeling was performed to determine whether the microvascular findings of FS-069 could explain its echocardiographic behavior when injected directly into a coronary artery.

Animal preparations. The dogs were anesthetized with 30 mg/kg of sodium pentobarbital (Abbott Laboratories), intubated and ventilated with a respirator pump (model 613, Harvard Apparatus). Additional anesthesia was administered during the experiment as needed. Leads were placed on the chest wall to obtain an electrocardiographic (ECG) signal. A 7F catheter was placed in the aorta to record pressure. A similar catheter was placed in the left femoral vein to administer fluids and drugs, as needed. Catheters were also placed in each femoral artery for duplicate reference sample withdrawal during radiolabeled microsphere injections and for sampling of arterial blood gases. A left lateral thoracotomy was performed, and the heart was suspended in a pericardial cradle.

The first part of the experiment consisted of measuring hemodynamic function, myocardial blood flow, left ventricular wall thickening and pulmonary gas exchange during repeated venous injections of FS-069. For this purpose, micromanometer-tipped 7F catheters (model TCB-500, Millar Instruments) were placed in the left atrium and left ventricle for the measurement of pressures. A 7F flotation catheter (Baxter-Edwards Laboratory) was placed in the pulmonary artery for measurement of pressures and connected to a computer (model 9520A, Edwards Laboratories) for measurement of thermodilution cardiac output. The fluid-filled aortic and pulmonary artery catheters were attached to fluid-filled transducers, which, in turn, were connected to a multichannel recorder (model ES2000, Gould Electronics). The catheters and the ECG leads were also connected to this recorder.

The second part of the experiment consisted of comparing the myocardial kinetics of FS-069 and Albunex during direct intracoronary injections. For this purpose, the proximal portion of the left anterior descending coronary artery was dissected free from the surrounding tissues. The right carotid artery was then exposed, and a 12F plastic cannula (model 1058, C.R. Bard Co.) was inserted into its lumen and secured in place with a tie. This cannula was connected to plastic tubing (Tygon, Norton Performance Plastics), whose opposite end was fastened to a custom-designed metal cannula. The tubing was then routed through a microcomputer-controlled peristaltic pump (model 2501, Harvard Apparatus), and the flow through it was measured using an extracorporeal time-of-flight ultrasonic flow probe (model 5C, Transonics) connected to a flowmeter (model T206, Transonics). The tubing was primed with blood from the carotid artery, and the left anterior descending coronary artery was ligated. The metal cannula attached to the tubing was inserted into the left anterior descending coronary artery distal to the site of ligation and was secured in place with a tie. A power injector (model 3000, Liebel-Flarsheim) was used for introduction of microbubbles into the tubing.

The microvascular rheology of FS-069 was compared to that of Albunex in the spinotrapezius muscle of the rat. Nine female Sprague-Dawley rats were anesthetized with an intramuscular injection of a mixture of 1% alpha-chloralose and 13.3% urethane at a dose of 0.6 ml/100 g of body weight. The right carotid artery was cannulated to enable injection of microbubbles. The right spinotrapezius muscle was prepared for intravital microscopy as previously described (14). The muscle was exteriorized, leaving the anterior edge with the main feeding artery and vein intact. The exposed muscle was continuously superfused with Ringer's solution (pH 7.4) warmed to 37°C and saturated with a 5% carbon dioxide and 95% nitrogen gas mixture. The muscle was spread over a transparent coverslip on a hollow pedestal to allow visualization with a microscope. After the dissection was complete, the preparation was allowed a minimum of 15 min to stabilize before observations were drawn.

Hemodynamic data acquisition. Hemodynamic data were acquired using the multichannel recorder, which was con-

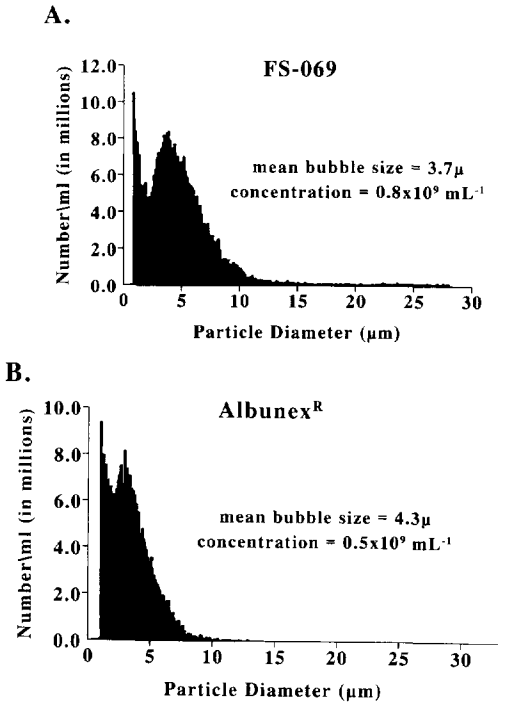

Figure 1. Size distributions and concentrations of **(A)** FS-069 and **(B)** Albunex.

nected to an 80386-based personal computer (model 2531, DTK Inc.) through an eight-channel analog-to-digital converter (DAS 16/16F, Keithley-Metrabyte). Data were acquired at 200 Hz and displayed in real time using data acquisition software (LabTech Notebook). These data were transferred to RS/1 (Bolt Beranek, and Newman), resident on a VAX-4000 (Digital Equipment Corp.) for later analysis. Five-second samples of the ECG and aortic, pulmonary artery, left atrial and left ventricular pressures were acquired at 20-s intervals before, during and after the FS-069 injection sequence. Left ventricular end-diastolic pressure and peak positive and negative left ventricular dP/dt were derived using a custom-designed program.

Two-dimensional echocardiography. Two-dimensional echocardiography was performed using a phased-array system with a 5-MHz transducer (RT5000, General Electric Medical Systems). Gain settings were optimized at the beginning of the experiment and were held constant throughout. A maximal dynamic range of 72 dB was used. A saline bath served as an acoustic interface between the heart and the transducer. Imaging was performed at the midpapillary muscle short-axis level with the transducer fixed in a permanent position by means of a clamp attached to the procedure table. Data were recorded on 1.25-cm S-VHS videotape using a S-VHS video recorder (Panasonic AG-7350, Matsushita Electric).

The optimal venous dose of FS-069 (Molecular Biosystems, Inc.) was determined in the closed chest animal (see protocol). A histogram of its size distribution is depicted in Figure 1A. For studying the effects on hemodynamic function, myocardial thickening and pulmonary gas exchange, FS-069 was administered intravenously using a programmable injector pump (model 22, Harvard Apparatus) at a rate of 0.3 ml/s at 20-s intervals. To compare the myocardial kinetics of FS-069 and Albunex after an intracoronary injection, the former was diluted in normal saline to a final dilution of 1:50. The myocardial kinetics of 0.25 ± 0.14 ml of diluted FS-069 was compared to those of 0.225 ± 0.12 ml of undiluted Albunex (Molecular Biosystems, Inc), the size distribution of which is depicted in Figure 1B. A saline flush was used with the injections so that the total volume injected was always 3 ml, and the injection rate was fixed at 1 ml/s for all intracoronary injections, resulting in identical input functions for each agent. Imaging was initiated a few seconds (5 to 10) before injection of microbubbles and was continued until after their visual disappearance from the myocardium.

Analysis of echocardiographic data. Echocardiographic images from the in vivo and in vitro experiments were transferred from videotape into the digital memory of an image processing workstation (Mipron, Kontron) and analyzed using custom-designed software (15). For the in vivo experiments, consecutive end-diastolic frames, beginning 4 to 5 frames before the appearance of contrast agent until after its clearance from the myocardium, were selected and aligned using cross correlation. The time-intensity data from intracoronary injections were fit to a gamma-variate function ($y = Ate^{-\alpha t}$) for Albunex and to the integral of the gamma-variate function ($y = A[1 - (1 + \alpha t)e^{-\alpha t}]$) for FS-069 (15). Venous injections of FS-069 were better suited to a gamma-variate fit. Images obtained at each concentration from the in vitro experiment were fit with the integral of a gamma-variate function.

At sampling times 4 min apart, three consecutive end-systolic and end-diastolic images were analyzed for left ventricular wall thickening. The epicardial and endocardial outlines of the left ventricle in these three sets of images were traced, and 64 equidistant points along these outlines were automatically defined and connected by the computer using a minimal distance rule. The percent wall thickening was calculated for each chord in each set of images using the equation: %wall thickening = (end-systolic chord length − end-diastolic chord length)/(end-diastolic chord length). The average thickening of all 64 chords from all three sets of images were used to derive the mean percent left ventricular wall thickening for each stage.

Myocardial blood flow measurement. Approximately 2×10^6 of 11-μm radiolabeled microspheres (Dupont Medical Products), suspended in 4 ml of 0.9% saline solution and 0.01% polysorbate 80 (Tween 80), was injected into the left atrium in a random order at 4-min intervals. Reference samples were withdrawn from the femoral artery over 130 s using a constant-rate withdrawal pump (model 944, Harvard Apparatus). At the end of the experiment, the heart was cut into ~250 pieces. Both these tissue samples and the arterial reference samples were counted in a well counter with a multichannel analyzer (model 1282, LKB Wallac). Corrections were made for activity spilling from one window to the next using a custom-designed computer program. Flow to each

sample was calculated using the equation: $Q_m = (C_m \times Q_r)/C_r$, where Q_m = myocardial flow (ml/min), C_m = tissue counts, Q_r = rate of arterial sample withdrawal (ml/min) and C_r = counts in the arterial reference sample (16). The average myocardial blood flow to the heart at each stage was calculated by averaging flows to all myocardial segments.

Blood gas analysis. Samples used for blood gas analysis were collected from the femoral artery through a 7F catheter 4-min apart. Approximately 2.0 ml of arterial blood was withdrawn using a glass syringe (3-ml Multifit, Becton-Dickinson) containing a small quantity of heparin sodium. The glass syringes were packed in an ice-filled container, and each sample was analyzed within 1 h of withdrawal using a blood gas and pH analysis machine (model 158, Ciba-Corning).

Intravital microscopy. The microvascular rheology of the microbubbles was studied with a high magnification microscope (Zeiss Customized ACM, Zeiss Inc.) mounted over the exteriorized spinotrapezius muscle preparation. A water immersion objective (×63) with numerical aperture (0.90 U) was used. The optical resolution of this system is 0.4 μm. Data were recorded using a video camera (model CCD-72, Dage-MTI Inc.) mounted on the microscope and connected to a S-VHS recorder (model AG-1730, Matsushita). An image intensifier (GenIIsys, Dage-MTI Inc.) resulted in a final magnification of ×2,200. Measurement were performed off-line using a video caliper (model 305R, Vista Electronics) with the images displayed on a high resolution (0.2 μm/line) monitor (model PVM-137, Sony Corp.).

In vitro experiment. An in vitro experiment was performed to determine whether the number of static microbubbles per tissue volume observed in the intravital microscopy studies was of a high enough concentration to account for the persistent myocardial opacification observed during echocardiography following intracoronary injections of FS-069. A glass beaker was filled with 4 liters of 0.9% saline solution. The echocardiographic transducer was fixed 2 cm into the saline near the center of the beaker to which various doses of FS-069 were introduced. A magnetic stirrer at the bottom of the beaker ensured thorough mixing of the microbubbles with the saline. Images were acquired for 10 s beginning at the time of injection and stored on videotape for later analysis.

Protocols. For determining the intravenous dose of FS-069 required for optimal myocardial opacification, closed chest echocardiographic examination was performed in the dogs before the lateral thoracotomy. FS-069 was injected in the femoral vein beginning at a dose of 0.3 ml with increments of 0.1 ml up to a maximal dose of 0.8 ml. Three minutes was allowed between injections for most of the agent to be cleared from the left ventricular cavity. From these injections, the optimal intravenous dose was determined for each dog based on the visual assessment of myocardial opacification, which was then used for all subsequent injections.

The dogs were then instrumented for the first part of the experiment, and beginning 4 min before the first injection of FS-069, continuous echocardiographic recording was initiated. Also beginning at this time, and at every minute thereafter, 5 s of hemodynamic data were sampled. Three minutes before the first injection of FS-069, radiolabeled microspheres were injected, blood samples were drawn for blood gas analysis and cardiac output was measured. These measurements were repeated at 4-min intervals. At time zero, FS-069 injections were initiated and repeated at 20-s intervals for 10 min. Hemodynamic data acquisition and echocardiographic recording ended 5 min after the last injection of FS-069. A single venous injection of FS-069 was given to study the myocardial kinetics of FS-069 from this route.

For the second part of the experiment, Albunex and FS-069 microbubbles were separately injected into the cannulated left anterior descending coronary artery at four different flow rates in each dog (ranging from 15 to 77 ml/min) to study their myocardial kinetics when injected through this route. At the end of the experiment, the heart was excised for myocardial blood flow analysis.

For intravital microscopy, both Albunex and FS-069 microbubbles were labeled with 90% DTAF (5-[(4,6-dichlorotriazin-2-YL)amino]-fluorescein (Sigma Chemical) as previously described (17). Before injecting the microbubbles, an area of the spinotrapezius muscle equal to 24 adjacent fields of view, each containing a clear view of the microvasculature throughout the tissue thickness, was previewed. Several transverse arteriole-collecting venule units were present within the region of observation; therefore, any potential biasing from topologic heterogeneity was negligible. The light source in the microscope was then switched from transillumination to epi-illumination at a peak wavelength of 510 nm, which is an appropriate excitation wavelength for DTAF. Approximately 0.17×10^9 microbubbles of Albunex or 0.30×10^9 microbubbles of FS-069 were injected into the carotid artery over 5 s. The number of static-labeled microbubbles in the previously mapped fields of view was then determined.

Statistical methods. Data are expressed as mean value ± 1 SD. Interstage comparisons were performed using repeated measures analysis of variance, and differences between individual stages were compared using the Student *t* test with the Bonferroni correction. Comparisons between echocardiographic and other measurements were made using linear regression analysis. Statistical significance was defined as $p < 0.05$ (two-sided).

Results

Effect of FS-069 on hemodynamic function, myocardial blood flow, left ventricular wall thickening and pulmonary gas exchange. Figures 2 and 3 summarize the effect of the 30 doses of FS-069 injected over 10 min (a dose every 20 s) on hemodynamic function, myocardial blood flow and pulmonary gas exchange. The variables are plotted beginning 3 min before the first injection of FS-069 to 5 min after the final injection. There were no significant changes in the mean aortic and pulmonary artery pressures (Fig. 2A), left atrial and left ventricular end-diastolic pressures (Fig. 2B) and peak positive and negative left ventricular dP/dt (Fig. 2C) over the 19 samples

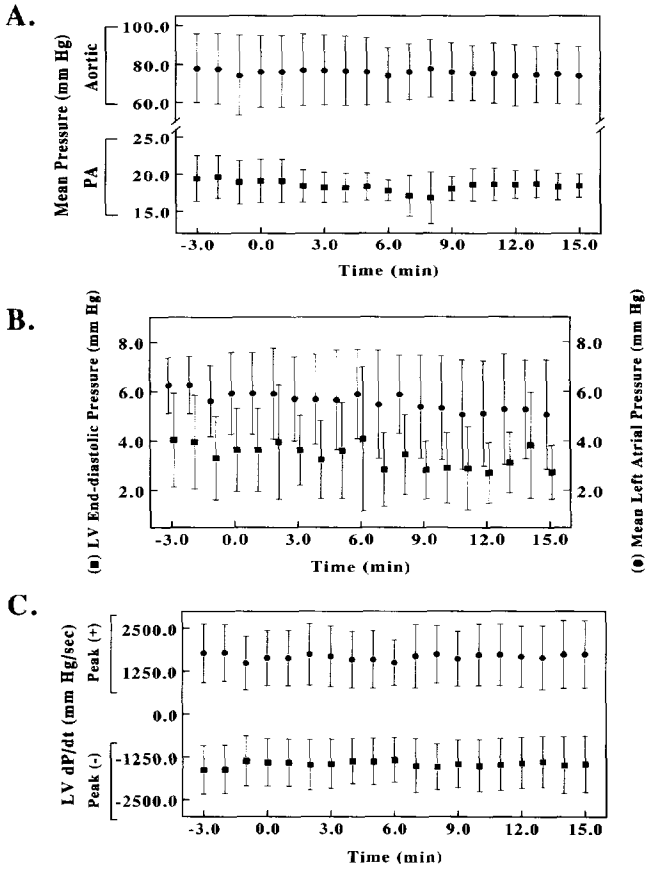

Figure 2. Effect of FS-069 injected every 20 s on mean aortic and pulmonary artery (PA) pressures (**A**), left ventricular (LV) end-diastolic and mean left atrial pressures (**B**) and peak positive and peak negative first derivative of left ventricular pressures (dP/dt) (**C**). These measurements were performed every 1 min starting 3 min before the first injection of FS-069 and continuing for 5 min after the last injection. See text for details.

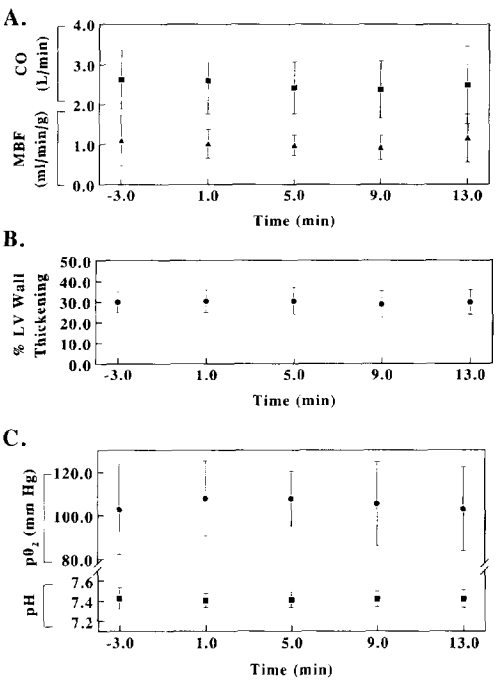

Figure 3. Effect of FS-069 injected every 20 s on cardiac output (CO) and myocardial blood flow (MBF) (**A**), percent left ventricular (LV) wall thickening (**B**) and partial pressure of oxygen (pO_2) and pH (**C**). These measurements were performed every 4 min starting 3 min before the first injection of FS-069 and continuing for 3 min after the last injection. See text for details.

obtained at 1-min intervals in all nine dogs. Similarly, no significant changes were found in the cardiac output and myocardial blood flow (left and right *y* axes, respectively, in Fig. 3A), echocardiographically determined percent left ventricular wall thickening (Fig. 3B), partial pressure of oxygen or pH (Fig. 3C). The partial pressure of carbon dioxide and HCO_3 also did not show significant changes. The mean cumulative dose of FS-069 for this part of the protocol in each dog was 15 ml. The mean dose required for myocardial opacification from venous injection was 0.5 ml.

Myocardial kinetics of FS-069. After venous injection, the myocardial kinetics of FS-069 approximated a gamma-variate form and indicated an unimpeded wash-in and wash-out of the bubbles throughout the myocardium. A direct injection of diluted FS-069 into the left anterior descending coronary artery, however, resulted in persistence of microbubbles within the myocardium. Figure 4A depicts data from one dog at four different flow rates. There is no relation between bubble wash-out and left anterior descending coronary artery flow. In comparison, as previously demonstrated (18), a direct intracoronary injection of Albunex resulted in time-intensity curves with a characteristic gamma-variate form and mean transit rates that correlated linearly with flow. Figure 4B illustrates Albunex time-intensity curves in the same dog using the same four flow rates as depicted in Figure 4A. A gradual disappearance of FS-069 microbubbles from the myocardium was noted over about 5 min. Similar results were obtained from all nine dogs.

Microvascular rheology of FS-069 versus Albunex. To better understand the persistence of FS-069 in the myocardium, the rheology of FS-069 was studied in the rat's spinotrapezius muscle using intravital microscopy. Of the nine rats, one died during preparation, one was injected with labeled Albunex only, three were injected with labeled FS-069 only and four were injected with labeled Albunex followed by labeled FS-069.

No bubble entrapment in the microcirculation was noted despite 10 injections of Albunex in five rats. When the procedure was repeated using FS-069, however, 1 to 15 static bubbles (mean 4.7, median 3) were found in the 24 fields of view after the first injection. In most cases, capillary vessels or small arterioles were observed to be "plugged" by a microbubble, as evidenced by the lack of erythrocyte flux in the vessel (Fig. 5). In a few cases, the plugs were found in small venules, typically at stagnation points in convergent bifurcations. Subsequent injections of FS-069 resulted in greater numbers of plugs.

The largest FS-069 microbubbles caused plugging. Of the

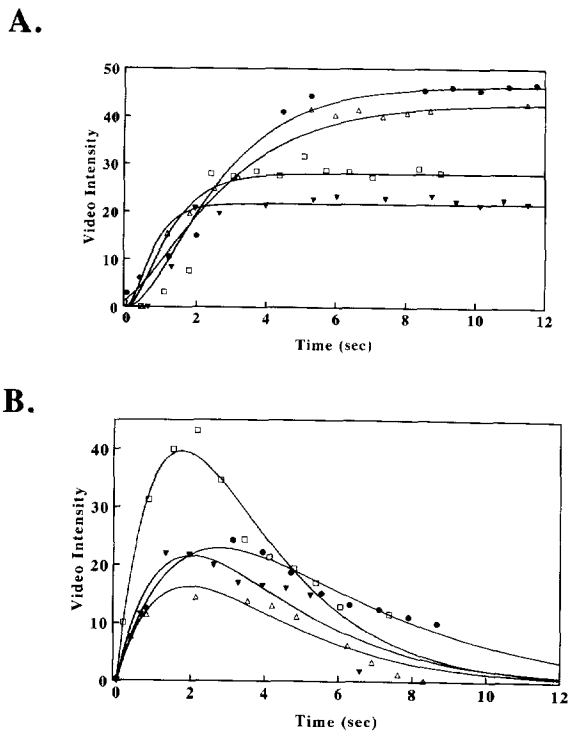

Figure 4. Time-intensity plots obtained from the anterior myocardium after direct left anterior descending coronary artery injections at four different flow rates in a group I dog using (**A**) diluted FS-069 and (**B**) diluted Albunex. See text for details. **Circles** = 20 ml/min; **solid triangles** = 70 ml/min; **squares** = 52 ml/min; **open triangles** = 35 ml/min.

104 plugs found, 33 of the most clearly focused, along with the microvessel containing them, were chosen for measurement: 28 were found to be elongated with a mean long-axis length (along the direction of the vessel) of 12.2 ± 2.9 μm. The maximal long-axis plug length recorded was 19.4 μm, whereas the minimum was 6.9 μm. The mean short-axis width (perpendicular to the vessel direction) was 9.4 ± 2.2 μm with maximal and minimal short-axis widths of 15.5 and 5.17 μm, respectively. The mean microvessel diameter containing these plugs was 6.1 ± 1.2 μm, which is consistent with normal measures of rat skeletal muscle capillary vessels (19). Microvessel diameters were measured as close as possible to the site of the plugged bubbles. Distention of the walls of the microvessel due to the lodged bubble was not uncommon. The mean amount of distention, determined by subtracting the diameter of the nondeformed vessel from the short-axis bubble width, was found to be 3.3 ± 2.1 μm.

Figure 5. Example of a field of view on intravital microscopy showing plugged FS-069 microbubbles at a magnification of ×1,375. The upper bubble had a short-axis diameter of 7.0 μm, a long-axis diameter of 7.4 μm and a vessel diameter of 5.2 μm. The lower bubble had a short-axis diameter of 7.9 μm, a long-axis diameter of 8.4 μm and a vessel diameter of 6.4 μm.

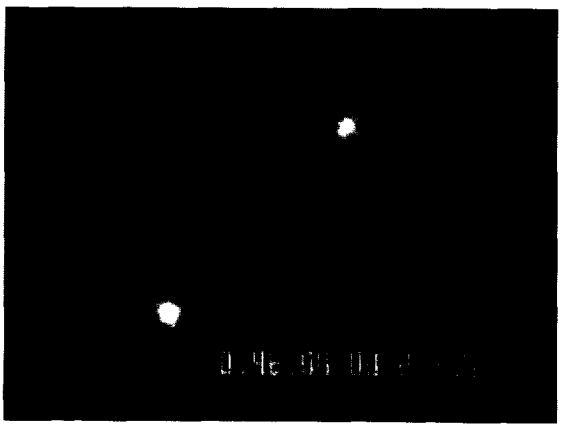

Results of in vitro modeling. Figure 6 (left) illustrates the nonlinear relation between microbubble concentration and video intensity for the echocardiographic system used in this study. To ascertain whether the prolonged myocardial opacification after intracoronary injection results from minimal plugging, calculations based on combined data from the intravital microscopy study and the in vitro experiment were performed. The diameter of a single field of view for the microscope used in the intravital observations (×63 objective) was 0.27 mm. Thus, the area of the field of view is

$$\frac{(0.27)^2\pi}{4} = 0.057 \text{ mm}^2$$

The average muscle thickness in the area used for our observations was 250 μm (0.250 mm) (20), so the volume of the tissue is 0.0143 mm^3 per field of view. A 6 × 4 region was scanned for each FS-069 injection; thus, the total volume corresponding to 24 fields of view is 0.3435 mm^3. If the mean number of plugs found in this volume of tissue is four, then the corresponding concentration of microbubbles in tissue can be determined as follows:

$$\frac{4 \text{ bubbles}}{0.3435 \text{ mm}^3} \times \frac{1{,}000 \text{ mm}^3}{1 \text{ cm}^3} \approx 11{,}644 \text{ bubbles/cm}^3$$

By applying this result to the concentration versus video intensity profile determined in the in vitro study (Fig. 6, left), one can see that the video intensity corresponding to this concentration of microbubble plugs is ~60 gray-scale units.

Discussion

Ideal properties of a venous echocardiographic contrast agent. The major determinant of backscatter from bubbles insonified at nonresonating frequencies is their size (11). It becomes obvious from Figure 6 (right), which depicts the relation between microbubble size and ultrasound backscatter, that even a small decrease in bubble size can result in a marked decrease in backscatter. There are many factors that can cause a decrease in bubble size, including the molecular weight and diffusibility of the gas contained in the microbubbles (10), the partial pressures of gases in the bubbles in relation to those of the same gases in blood (21) and the ambient pressure in the in vivo system (22). The first-generation contrast agents, such as Albunex, are most susceptible to these factors. The gases

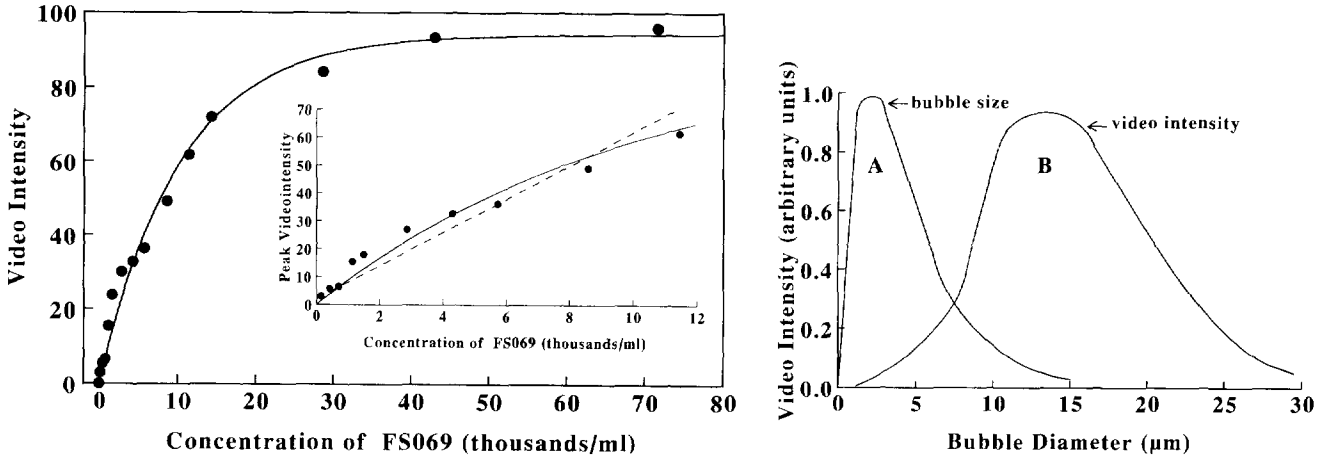

Figure 6. Left, Relation between microbubble concentration of bubbles versus video intensity that demonstrates why a small number of microbubbles entrapped in tissue can result in a bright and persistent contrast effect. **Right,** Relation between microbubble size and backscatter. **Curve A** = size distribution of microbubbles (αde^{-dk}; k = 0.5; average d = 4 μm). **Curve B** = backscatter [$\alpha(de^{-dk})d^6$] (11).

contained in these bubbles (mainly nitrogen and oxygen) are highly diffusible and soluble and leak out of the bubbles when they are mixed with blood, thus decreasing their size and backscatter. Consequently, conditions associated with prolonged pulmonary transit of the bubbles, such as a low cardiac output (23), result in lesser contrast effect in the left ventricular cavity after a venous injection of these bubbles.

FS-069 is a modification of Albunex containing perfluoropropane, a high molecular weight gas that is less diffusible than air (10). The concentration of microbubbles in FS-069 is almost twice that of Albunex, and it also has a greater proportion of larger bubbles (Fig. 1). This agent consistently produces myocardial opacification irrespective of the duration of contact with blood (12,13). As noted in our study, the dose of FS-069 required for optimal myocardial opacification from a venous injection in the dog is ~0.5 ml.

Successful transpulmonary passage is essential for a venous contrast agent to opacify the left heart, and bubbles larger than the pulmonary capillary vessels cannot cross the lungs. A high concentration of large bubbles can also cause pulmonary microcirculatory blockage, resulting in hypoxia, increased pulmonary vascular resistance and decreased forward flow (cardiac output). For this reason these variables were measured in our study. Despite 30 rapidly injected consecutive doses, each adequate to cause myocardial opacification, there were no changes in pulmonary gas exchange, pulmonary artery pressure or cardiac output, indicating that any larger bubbles present in FS-069 and trapped within the pulmonary microcirculation are too sparse to cause any changes in these variables.

Once the bubbles traverse the lungs and enter the left heart, they should not cause any changes in systemic and cardiac hemodynamic function. Despite 30 consecutive rapid doses of FS-069, no changes in aortic pressure or peak positive and negative left ventricular dP/dt were noted. Additionally, no changes in radiolabeled microsphere–measured myocardial blood flow were seen. These results indicate that the bubbles, after pulmonary transit, do not cause microcirculatory imbalances within the myocardium. The lack of any effect on left ventricular wall thickening also supports the absence of any direct myocardial depressant effect or any indirect effect on myocardial mechanics modulated through abnormalities induced in myocardial blood flow.

Myocardial kinetics of microbubbles. There are two main approaches that can be used to measure myocardial perfusion using tracers that reside entirely within the intravascular space (24). One approach is using a deposit tracer that becomes completely entrapped within the microcirculation, as is the case with radiolabeled microspheres that are lodged within the arterioles (16). The number of microspheres per unit of tissue then provides an estimate of flow to that tissue. This approach is currently impractical for myocardial contrast echocardiography using venous injection, because bubbles large enough to be entrapped in the coronary arterioles cannot cross the lungs. The number of microbubbles that get entrapped within the arterioles required to produce a contrast effect on echocardiography in closed chest humans may also be large enough to cause significant hemodynamic effects. Although rest myocardial blood flow may not be affected by entrapment of bubbles in normal subjects because of the abundant coronary flow reserve, it may have adverse effects in patients with coronary artery disease who have partial or complete exhaustion of flow reserve. It is conceivable that with more sensitive ultrasound methods such as harmonic imaging (25,26), significantly fewer bubbles may be required within the myocardium to produce adequate opacification, allowing measurement of myocardial blood flow from a direct left heart injection of bubbles that are fully entrapped within the myocardial microcirculation.

The second approach for measuring myocardial blood flow is using tracers that freely traverse the microcirculation and recording their transit through tissue. Variables of time-intensity curves thus obtained can then be used to measure myocardial perfusion (flow and volume) (18,24). It appears

from our study that when FS-069 is injected intravenously, its transit through the myocardium simulates a gamma-variate form. When injected directly into the coronary artery, however, persistence of myocardial opacification is noted. To better understand the differences in myocardial kinetics of FS-069 when injected intravenously and into the coronary artery, we studied this agent using intravital microscopy and compared it with Albunex. We previously demonstrated that Albunex microbubbles have an intravascular rheology similar to that of red blood cells, both during intravital microscopy (17) and when these bubbles are injected directly into the coronary artery (18). As expected, we found that Albunex microbubbles were not trapped in the microcirculation of the rat's spinotrapezius muscle. Although the majority of the diluted FS-069 microbubbles also was not trapped, a few larger bubbles were. In vitro modeling confirmed that the persistent myocardial opacification seen after coronary injections can occur from the plugging of the microcirculation by a few bubbles.

These results explain the disparate myocardial kinetics of FS-069 when injected intravenously versus into the coronary artery. Unlike the intracoronary setting, the relatively larger bubbles are likely filtered by the lungs when injected intravenously. As shown in Figure 1, larger bubbles are more common in FS-069 than in Albunex, which may explain the differences in myocardial kinetics of the two agents when injected into the coronary artery. The few large bubbles present in Albunex may either be destroyed during injection or become smaller after contacting blood. Their absence in the microcirculation studies and in the myocardium during arterial injections supports these possibilities.

Our results also indicate that direct coronary injections of FS-069 are unlikely to provide information on myocardial blood flow. They are not suitable as deposit tracers because they are not all trapped within the myocardium. Tracer kinetics also cannot be used with these bubbles to determine myocardial blood flow because a few of them cause persistent opacification, precluding the assessment of time-intensity data. Because only a few of the bubbles are lodged within the myocardium, they are unlikely to cause harmful effects. Because they reside within the myocardium for several minutes, they could provide information on the spatial distribution of myocardial perfusion. Although Albunex is superior in terms of assessing myocardial blood flow after a direct bolus injection into the coronary artery (18,27), its transit through the myocardium under these conditions may be too rapid to provide an adequate on-line assessment of the spatial distribution of myocardial perfusion.

Study limitations. Ultrasound was used in this study 1) to determine the optimal dose of FS-069 required for adequate myocardial opacification from a venous injection in a close-chest dog; 2) to measure the effect of FS-069 on left ventricular wall thickening; and 3) to study the myocardial kinetics of FS-069 and Albunex. Microbubbles are destroyed by ultrasound when they are insonified at their resonating frequency (25,26). We have shown that FS-069 microbubbles are destroyed at frequencies of 2 to 3 MHz, with little or no destruction at frequencies of 5 MHz or higher (26). The use of a 5-MHz transducer, therefore, allowed us to study microbubbles both in vivo and in vitro without destroying them. We also recently found that a venous injection of 0.5 ml of FS-069 is more than adequate for myocardial perfusion in humans during intermittent harmonic imaging (13). We studied the hemodynamic effects of multiple injections of FS-069 in this study because in the clinical setting multiple injections are likely to be performed for image acquisition in different views both before and after interventions. Although Albunex has been approved by the Food and Drug Administration as a venous agent, one of its off-label applications is intracoronary injections (28), for which it has been shown to be safe in both dogs and humans (29,30). The safety of intracoronary injections of FS-069 has not been studied.

Conclusions. This study describes the effects of FS-069, a new second-generation echocardiographic contrast agent, on cardiac and systemic hemodynamic function, myocardial blood flow, left ventricular wall thickening and pulmonary gas exchange during and after venous injections of 30 consecutive doses performed every 20 s. It also characterizes the myocardial kinetics of this agent when injected both intravenously and into the coronary artery and explains why this agent, unlike Albunex, cannot provide information on myocardial blood flow when it is injected into the coronary artery. This study also provides a framework for the evaluation of other new echocardiographic contrast agents that are being developed and will be developed in the future.

We acknowledge the assistance of Suad Ismail, MD, during conduction of the in vivo experiments, and the helpful critique of the manuscript by Jonathan Lindner, MD.

References

1. Kaul S, Glasheen W, Ruddy TD, Pandian NG, Weyman AE, Okada RD. The importance of defining left ventricular "area at risk" in-vivo during acute myocardial infarction: an experimental evaluation utilizing myocardial contrast 2D-echocardiography. Circulation 1987;75:1249–60.
2. Villanueva FS, Glasheen WP, Sklenar J, Kaul S. Assessment of risk area during coronary occlusion and infarct size after reperfusion with myocardial contrast echocardiography using left and right atrial injections of contrast. Circulation 1993;88:596–604.
3. Sabia PJ, Powers ER, Jayaweera AR, Ragosta M, Kaul S. Functional significance of collateral blood flow in patients with recent acute myocardial infarction. A study using myocardial contrast echocardiography. Circulation 1992;85:2080–9.
4. Sabia PJ, Powers ER, Ragosta M, Sarembock IJ, Burwell LR, Kaul S. An association between collateral blood flow and myocardial viability in patients with recent myocardial infarction. N Engl J Med 1992;372:1825–31.
5. Ragosta M, Camarano G, Kaul S, Powers E, Sarembock IJ, Gimple LW. Microvascular integrity indicates myocellular viability in patients with recent myocardial infarction: new insights using myocardial contrast echocardiography. Circulation 1994;89:2562–9.
6. Villanueva FS, Glasheen WP, Sklenar J, Kaul S. Characterization of spatial patterns of flow within the reperfused myocardium using myocardial contrast echocardiography: implications in determining the extent of myocardial salvage. Circulation 1993;88:2596–606.
7. Ismail S, Jayaweera AR, Goodman NC, Camarano GP, Skyba DM, Kaul S. Detection of coronary artery stenoses and quantification of blood flow

mismatch during coronary hyperemia with myocardial contrast echocardiography. Circulation 1995;91:821–30.

8. Villanueva FS, Spotnitz WD, Jayaweera AR, Gimple LW, Dent J, Kaul S. On-line intraoperative quantitation of regional myocardial perfusion during coronary artery bypass graft operations with myocardial contrast two-dimensional echocardiography. J Thorac Cardiovasc Surg 1992;104:1524–31.
9. Villanueva FS, Spotnitz WD, Glasheen WP, Kaul S. New insights into the physiology of retrograde cardioplegia delivery comparison with anterograde delivery. Am J Physiol 1995;268:H1555–66.
10. Porter T, Xie F, Kilzer K. Intravenous perfluoropropane-exposed sonicated dextrose albumin produces myocardial contrast which correlates with coronary blood flow. J Am Soc Echocardiogr 1995;8:710–8.
11. Albers VM. Underwater Acoustic Handbook. Hershey (PA): Pennsylvania State University Press, 1960.
12. Firschke C, Lindner JR, Wei K, Goodman NC, Kaul S. Detection of coronary stenoses using venous injection of FS-069 with intermittent harmonic imaging [abstract]. J Am Soc Echocardiogr 1996;9:362.
13. Senior R, Lahiri A, Raval U, Khattar R, Dittrich H, Kaul S. Detection of coronary artery disease using myocardial contrast echocardiography: comparison with ^{99m}Tc-sestamibi single photon emission computed tomography [abstract]. Circulation. In Press.
14. Gray SD. Rat spinotrapezius muscle preparation for microscopic observation of the terminal vascular bed. Microvasc Res 1973;5:395–400.
15. Jayaweera AR, Matthew TL, Sklenar J, Spotnitz WD, Watson DD, Kaul S. Method for the quantitation of myocardial perfusion during myocardial contrast two-dimensional echocardiography. J Am Soc Echocardiogr 1990: 3:91–8.
16. Heyman MA, Payne BD, Hoffman JI, Rudolf AM. Blood flow measurements with radionuclide-labeled particles. Prog Cardiovasc Dis 1977;20:52–79.
17. Keller MW, Segal SS, Kaul S, Duling B. The behavior of sonicated albumin microbubbles within the microcirculation: a basis for their use during myocardial contrast echocardiography. Circ Res 1989;65:458–67.
18. Jayaweera AR, Edwards N, Glasheen WP, Villanueva FS, Abbott RD, Kaul S. In-vivo myocardial kinetics of air-filled albumin microbubbles during myocardial contrast echocardiography: comparison with radiolabeled red blood cells. Circ Res 1994;74:1157–65.
19. Skalak TC, Schmid-Schonbein GW. The microvasculature in skeletal muscle iv. A model of the capillary network. Microvasc Res 1986;32:333–47.
20. Mazzoni MC, Skalak TC, Schmid-Schonbein GW. Effects of skeletal muscle fiber deformation on lymphatic volume. Am J Physiol 1990;259:H1860–8.
21. Wibble JH, Wojdyla JK, Bales GL, McMullen WN, Geiser EA, Buss DD. Inhaled gases affect the ultrasound contrast produced by Albunex in anesthetized dogs. J Am Soc Echocardiogr 1996;9:442–51.
22. Vuille C, Nidorf M, Morrissey RL, Newell JB, Weyman AE, Picard MH. Effect of static pressure on the disappearance rate of specific echocardiographic contrast agents. J Am Soc Echocardiogr 1994;7:347–54.
23. Galanti G, Jayaweera AR, Villanueva FS, Glasheen WP, Ismail S, Kaul S. Transpulmonary transit of microbubbles during contrast echocardiography: implications for estimating cardiac output and pulmonary blood volume. J Am Soc Echocardiogr 1993;6272–8.
24. Lindner JR, Kaul S. Insights into the assessment of myocardial perfusion offered by the different currently used cardiac imaging modalities. J Nucl Cardiol 1995;2:446–60.
25. Porter TR, Xie F. Transient myocardial contrast after initial exposure to diagnostic ultrasound pressures with minute doses of intravenously injected microbubbles. Demonstration of potential mechanisms. Circulation 1995;92: 2391–5.
26. Wei K, Skyba DM, Firschke C, Lindner JR, Jayaweera AR, Kaul S. Why are bubbles destroyed by ultrasound? [abstract] Circulation. In Press.
27. Ismail S, Jayaweera AR, Camarano G, Gimple LW, Powers ER, Kaul S. Relation between Air-filled Albumin Microbubble and Red Blood Cell Rheology in the Human Myocardium: Influence of Echocardiographic Systems and Chest Wall Attenuation. Circulation 1996;94:445–51.
28. Bach DS, Muller DWM, Cheirif J, Armstrong W. Regional heterogeneity on myocardial contrast echocardiography without severe obstructive coronary artery disease. Am J Cardiol 1995;75:982–6.
29. Keller MW, Glasheen WP, Kaul S. Albunex: a safe and effective commercially produced agent for myocardial contrast echocardiography. J Am Soc Echocardiogr 1989;2:48–52.
30. ten Cate FJ, Widimsky P, Cornel JH, Waldstein DJ, Serruys PW, Waaler A. Intracoronary Albunex. Its effect on left ventricular hemodynamics, function, and coronary sinus flow in humans. Circulation 1993;88:2123–7.